Ultra-short wavelength operation of thulium-doped fiber amplifiers and lasers

Shaoxiang Chen[1*, 2], Yongmin Jung[1], Shaif-ul Alam[1], David J. Richardson[1], Raghuraman Sidharthan[2], Daryl Ho[2], Seongwoo Yoo[2] and Jae M. O. Daniel[3]**

[1]*Optoelectronics Research Centre, University of Southampton, SO17 1BJ, United Kingdom*
[2]*School of Electrical and Electronic Engineering, The Photonics Institute, Nanyang Technological University, Singapore 639798*
[3]*Aether Photonics, Sydney, Australia*
*sc4f15@soton.ac.uk, **Chen0976@e.ntu.edu.sg

Abstract: We fabricate and characterize a germanium/thulium (Ge/Tm) co-doped silica fiber in order to enhance the gain at the short wavelength edge of the thulium emission band (i.e. 1620-1660 nm). The Ge/Tm doped fiber shows an intrinsic blue-shifted absorption/emission cross-section compared to aluminum/thulium (Al/Tm) co-doped fiber, which greatly improves the short wavelength amplification and has enabled us to further extend the shortest wavelength of emission towards 1600 nm. Using this glass fiber composition, we have demonstrated both a silica-based thulium doped fiber amplifier (TDFA) in the 1628-1655 nm waveband and a tunable thulium-doped fiber laser (TDFL) capable of accessing the telecom U-band wavelength region. These results represent by far the shortest amplifier/laser wavelengths reported to-date from TDFAs/TDFLs.

1. Introduction

The broadband fluorescence of thulium-doped silica glass across the 1600-2200 nm waveband offers great potential for the development of active fiber gain media for power scalable fiber lasers and optical amplifiers in the near-infrared region [1]. To date, most research efforts have been devoted to lasers operating in the wavelength region 1750-2050 nm (near the emission peak of the Tm^{3+} ion). This is because achieving efficient optical amplifier/laser operation in the 1600-1750 nm region (i.e. short wavelength edge of Tm emission) is very challenging due to the quasi-three-level nature of the $^3F_4$ -$^3H_6$ transition which necessitates a high population inversion to achieve appreciable gain and effective suppression of long wavelength amplified spontaneous emission (ASE). However, fiber laser systems operating in this spectral region are very attractive for a range of applications including light detection and ranging (LIDAR), medicine, optical sensors, spectroscopy and telecommunications. This spectral range not only falls in the atmospheric transparency window, but it also offers eye safety because the maximum permissible laser exposure at the cornea of the human eye is much higher ($>10^4$) than that at wavelengths around 1060 nm (i.e. serviced by ytterbium doped fiber lasers) and therefore such lasers are ideally suited for remote sensing, detection and LIDAR applications. Furthermore, the use of laser radiation at 1650 nm for eye surgery gives a higher penetration depth and improved incision quality as demonstrated by Crotti et al. [2], whilst being considered eye-safe. Moreover, the optimum operating wavelength window for deep-tissue imaging lies in the 1600-1700 nm region due to improved tissue penetration when considering tissue scattering and absorption effects [3-5]. In addition, tunable sources operating around 1650 nm are of particular interest for methane sensing due to its strong absorption lines spanning from 1635 nm to 1675 nm [6-8]. Finally, as the low-loss transmission window of silica fiber extends up to 1700 nm (attenuation ~0.5 dB/km @1700 nm), operation of optical amplifiers in the 1620-1700 nm range is of potential interest in telecommunications because they could potentially fill the

gap between the extended L-band erbium-doped fiber amplifier (EDFA) and the state-of-the-art TDFAs as illustrated in Fig. 1.

However, to date, there is no practical rare earth doped fiber amplifier and/or laser for the 1620-1700 nm region. Bismuth-doped germanosilicate fibers (BDGF) have the potential to operate over the 1620-1700 nm window, however they exhibit low efficiency and most importantly the origin of the near infrared emission of bismuth is still not properly understood, which is currently hindering further improvements in BDGF amplifiers [9]. Fluoride glass based TDFs with a W-type index profile [10] have been proposed theoretically as a potential gain fiber to access this region and a Tm/Tb co-doped fluoride fiber laser has been experimentally demonstrated down to 1636 nm [11]. However, fluoride glass fibers are very difficult to handle, are generally hygroscopic and are difficult to integrate with silica-based components and systems.

In order to improve the short wavelength operation of silica-based Al/Tm co-doped fiber, Daniel et al. proposed a low-loss laser cavity using a high reflectivity fiber Bragg grating (FBG), whereby a shortest lasing wavelength of 1660 nm was achieved [12]. However, the lasing efficiency at 1660 nm in these experiments could not be determined due to the high threshold pump power [12]. Intriguingly, Barnes et al. have reported the possibility of achieving a TDFL at 1650 nm by using Ge/Tm co-doped fiber, which provides preferential gain at short wavelengths as compared to Al/Tm-doped fiber, however the shortest emission wavelength achieved from their Ge/Tm fiber was 1700 nm [13]. In addition, Agger et al. have reported that Al/Ge/Tm co-doped fiber has a blue-shifted absorption- and emission cross section compared to those of Al/Tm co-doped fiber [14], but they did not provide a demonstration of fiber amplifiers or lasers using this fiber.
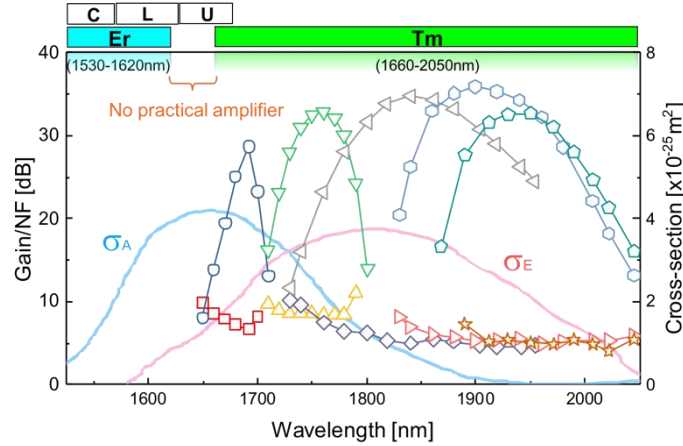

Fig. 1. The gain and noise figure of TDFAs demonstrated by using Al/Tm co-doped fiber [15], with its corresponding absorption- (σ_A) and emission cross section (σ_E), respectively [14].

Over the last 7 years, we have demonstrated several different architectures to achieve high performance TDFAs covering wavelengths from 1650 to 2050 nm using commercially available Al/Tm co-doped fiber (OFS TmDF200). A summary of the combined gain/noise figure (NF) of our various TDFAs is provided in Fig. 1. By suppressing the ASE at the longer wavelengths, we managed to extend the spectral gain coverage of the TDFA to the 1650-1700 nm wavelength range, achieving a small signal gain of up to 29 dB at 1690 nm [16]. Note that the peak absorption cross section (σ_A) of Al/Tm co-doped fiber is located around 1650 nm and that the absorption cross section is much higher than the emission cross section (σ_E) below 1650 nm. Therefore, realizing efficient laser/amplifier operation below 1650 nm is extremely challenging and intrinsically limited by the host glass used.

In order to realize efficient fiber amplifier/laser systems operating below 1650 nm, we explore a different host glass composition, specifically Ge/Tm co-doped fiber. Our initial

results indicate that the Tm^{3+} absorption/emission peaks can be successfully blue-shifted with this glass composition. Based on the spectroscopic characteristics of Ge/Tm co-doped fiber, we experimentally demonstrate ultra-short wavelength operation of a TDFA and present the first realization of a silica-based TDFA operating down to a wavelength as short as 1628 nm. Also, we present the first demonstration of a tunable TDFL operating over the 1620-1660 nm wavelength range, which extends the operational range of thulium doped silica fibers down to the long wavelength edge of the L-band EDFA. Our results represent by far the shortest laser wavelengths ever reported from a silica-based TDFL.

2. Fiber fabrication and spectroscopy

Our Ge/Tm co-doped fiber was fabricated in-house using the modified chemical vapor deposition (MCVD) technique in conjunction with solution doping (representative dopant concentrations of ~0.12 wt. % for Tm and ~19 wt. % for Ge as shown in Fig. 2(a)). The fiber has a core diameter of 4.4 μm and a numerical aperture of ~0.28. Due to the Al^{3+} free environment, the Tm^{3+} concentration was kept relatively low in our Ge/Tm co-doped fiber in order to avoid any undesirable problems with clustering [17]. Moreover, Ge with four-coordinated structure is similar to the fused silica, thus providing the Tm^{3+} ions an approximate pure silica environment in germanosilicate glass as compared with alumino-silicate glass. In addition, the peak absorption wavelength in the $_3F^4$ manifold has the trend of shorter-wavelength shift with reduction of Al_2O_3 concentration in Al/Tm co-doped fiber [18]. In order to determine the primary spectroscopic properties of the fabricated Ge/Tm co-doped fiber the absorption spectra of both the Ge/Tm and Al/Tm co-doped fiber were measured by the cutback method using a supercontinuum source (Fianium WhiteLase) and an optical spectrum analyzer (OSA, Yokogawa AQ6375). As shown in Fig. 2(b), the absorption spectrum of the Ge/Tm co-doped fiber is significantly blue-shifted (~70 nm shorter) compared to that of the commercial Al/Tm co-doped fiber (OFS TmDF200), with a peak absorption of 20 dB/m at 1580 nm. The full-width at half-maximum (FWHM) of the absorption band of the $^3F_4$ manifold is also narrowed (~20 nm) compared to that of the Al/Tm co-doped fiber.
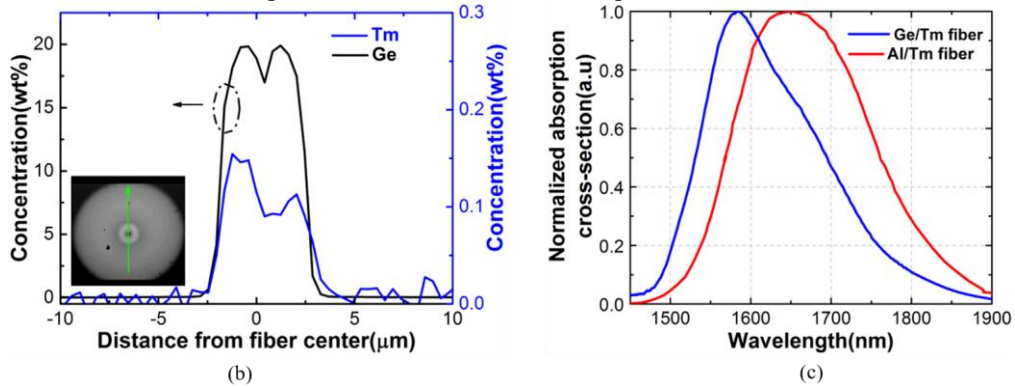

(b)

(c)

Fig. 2. (a) Measured doping concentration of a representative fabricated Ge/Tm co-doped fiber using an electron probe micro-analyzer (along the direction of the green arrow as shown in the inset), (b) the normalized absorption cross-section of the Al/Tm co-doped fiber and our in-house fabricated Ge/Tm co-doped fiber, respectively.

According to McCumber theory [19], the derived emission cross-section of the Ge/Tm co-doped fiber is also blue-shifted by ~40 nm as compared to that of the Al/Tm co-doped fiber, as shown in Fig. 3(a). Therefore, it is to be anticipated that the proposed Ge/Tm co-doped fiber can be used for efficient signal amplification at wavelengths much shorter than 1650 nm. Using the derived absorption and emission cross sections, the net gain coefficient G(λ) can be estimated by the following equation [20]:

$$G(\lambda) = \rho_0[p\sigma_e(\lambda) - (1-p)\sigma_a(\lambda)] \qquad (1)$$

where ρ_0 represents the Tm-doping concentration in the core, and p represents the population fraction of the upper $^3F_4$ laser level. This expression for the net gain coefficient as a function of population inversion is helpful in gaining insight into the short wavelength gain spectra for different levels of pumping. As shown in Fig. 3(b), the gain spectrum strongly depends on the population inversion and a high population inversion is required to achieve positive gain at shorter wavelengths. For example, to achieve signal amplification below 1650 nm, a population inversion of more than 60 % is needed, which is a great improvement as compared to previous reports on Al/Tm co-doped fiber where a population inversion of >80% is anticipated in order to achieve gain at such short wavelengths [12].

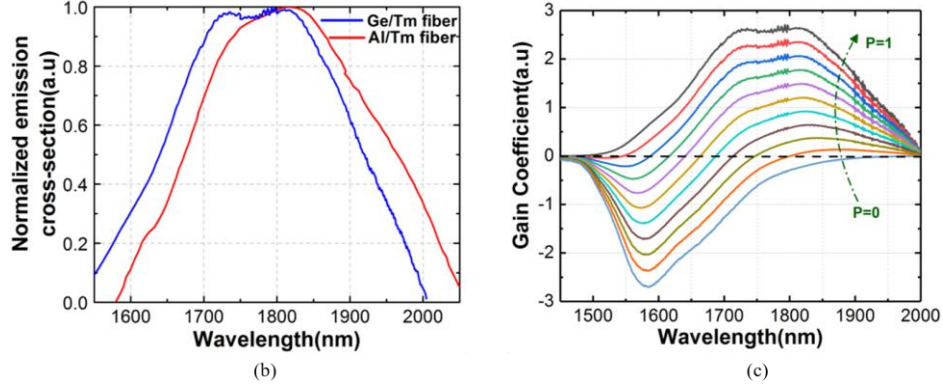(b)   (c)

Fig. 3. (a) Normalized emission cross-sections for Al/Tm co-doped fiber and in-house fabricated Ge/Tm co-doped fiber, respectively, and (b) the calculated normalized gain coefficient of Ge/Tm co-doped fiber at different population inversion levels.

3. Experiments and results

We undertook a range of amplifier and laser experiments using different lengths of the fabricated Ge/Tm co-doped fiber ranging from 2-6m and it was found experimentally that a 4.5m fiber length provided the maximum signal gain at the shortest emission wavelength whilst minimizing the reabsorption loss as described below. An in-house built 1565 nm all-fiber continuous wave (CW) pump laser was used to pump the active fiber.

3.1 Short wavelength TDFA operation

Figure 4(a) shows a schematic of our short wavelength TDFA. In our experiment, a double-pass amplifier configuration (whereby the signal to be amplified passes the gain region twice) was used with a high reflectivity FBG and a circulator to better exploit the available population inversion and thereby enhance the gain performance of the amplifier. Here, the high reflectivity FBG serves as a signal retroreflector to realize the double pass cavity and also as an efficient ASE filter to help reject long-wavelength ASE from the amplifier. The FBG is mechanically coupled to a compressible body to allow its peak reflectivity wavelength to be tuned from 1620 nm through to 1660 nm using an axial compression mechanism [21]. The measured reflectivity and bandwidth of the FBG varied from 91 % to 94 % and from 0.67 nm to 1 nm, respectively, depending on the operating wavelength. A commercially available tunable laser source (Tunics T100S-HP) covering the wavelength range 1500-1680 nm was used as a seed laser and an optical circulator (optimized for performance at 1650 nm with >40 dB optical isolation and 0.45 dB insertion loss) was employed to separate the input signal from the amplified output signal of the double-pass amplifier. A thin-film filter based 1565/1650 nm wavelength division multiplexing (WDM) coupler was used to combine the signal and pump signals. The insertion loss of the WDM coupler was less than 2 dB but this gradually increased at shorter wavelengths (e.g. 1.4 dB at 1640 nm and 3.1 dB at 1630 nm). Moreover, a 1565 nm FBG with ~99 % reflectivity was incorporated to recycle the residual pump light (~0.4 W for a launched pump power of 4.85W). Also, note that our fabricated Ge/Tm co-doped fiber exhibits a large mode

field diameter mismatch with conventional single mode fiber (SMF-28). A short segment of intermediate fiber (OFS TmDF200) was therefore spliced between the two fibers to reduce the overall splice loss to ~0.8 dB (as measured at a wavelength of 1300nm where the signal absorption is low).The optical spectrum and output power of the amplifier were measured by an optical spectrum analyzer and a thermal power meter (Ophir 3A-FS), respectively, enabling the external gain and NF to be evaluated.

(a)

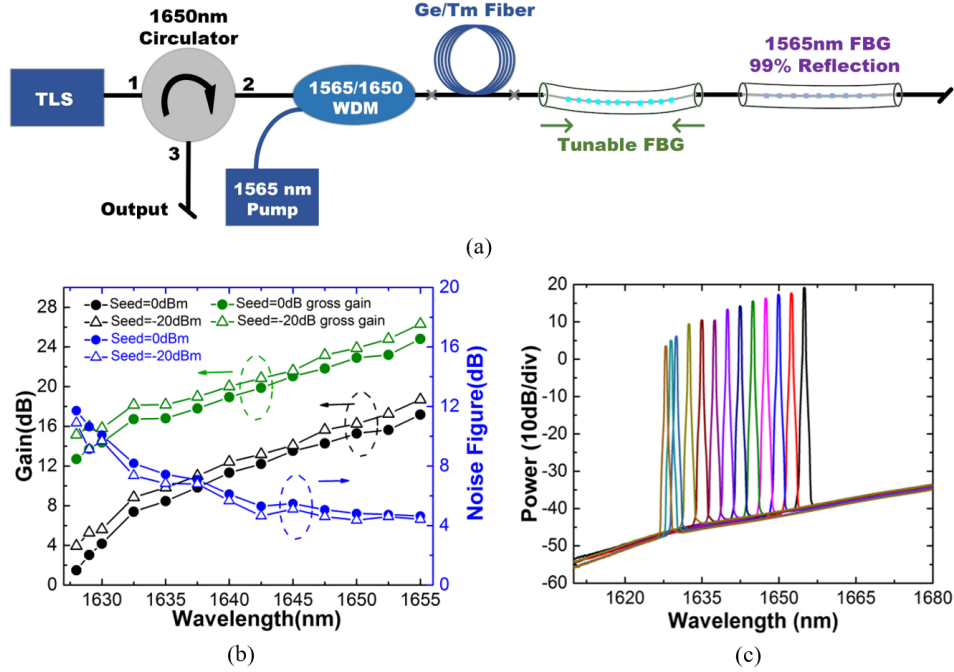(b)   (c)

Fig. 4. (a) Schematic of a short-wavelength TDFA, TLS: tunable laser source, (b) gain and NF performances of the TDFA, and (c) amplified spectra for saturated signals, measured with 0.1 nm OSA resolution.

Table 1. Main characteristics of TDFAs, BDFA and Raman fiber amplifier at 1650nm

Parameter	TDFA (Silica-based glass)		TDFA	BDGF amplifier	Raman fiber amplifier
	(Al/Tm fiber)	(Ge/Tm fiber) [present work]	(Tb/Tm fluoride fiber)	(Bismuth-doped germania fiber)	(Tellurite fiber)
Pump power, dBm	37.00	36.86	24.42	24.77	30.37
Pump source, nm	1565nm fiber laser	1565nm fiber laser	1210nm laser diode (LD)	1550nm LD	4-wavelength-channel pump LDs
Fiber length, m	1	4.5	14	50	250
Small signal gain @1650nm, dB	8	16.5	~4	~5	~10
Noise figure @1650nm, dB	10	4.4	~6.5	~9	~5.8
Gain coefficient @1650nm, dB/mW	0.0016	0.0034	0.0144	0.0167	0.0092

Figure 4(b) shows the gain and NF performance of the TDFA with respect to the launched pump power of ~4.85 W from 1565 nm CW fiber laser. Two different input signal powers were used as a representative small signal (-20 dBm) and saturated signal (0 dBm) gain in the 1628-1655 nm region and the external small-signal/saturated gain and NF values are determined by

the retrieved spectra from OSA (Yokogawa AQ6375). An external small-signal gain of 18.7 dB was achieved at 1655 nm, 8.8 dB at 1632 nm and 4.0 dB at 1628 nm. Compared to our previous demonstration of a short-band TDFA based on Tm/Al co-doped fiber [16], we have successfully extended the short wavelength edge of the silica-based TDFA from 1650 nm to 1628 nm. The saturated gain is above 7.0 dB in the 1632-1655 nm waveband, with up to 17.2 dB saturated gain achieved at 1655 nm. The external NFs for saturated signal and small signal were as low as 4.6 dB and 4.4 dB at a wavelength of 1655 nm but increased towards shorter wavelengths. This is mainly due to the insertion loss characteristics of the WDM coupler used and strong re-absorption of signal light by Tm^{3+} ions in their ground state. By considering the total insertion loss of our amplifier (particularly, the WDM coupler loss) in this double pass architecture, the gross (internal) small-signal gain was determined to be around 15-26 dB in the 1628-1655 nm range. Figure 4(c) shows amplified optical spectra for a saturated signal with over 50 dB in-band optical signal to noise ratio (OSNR) across the entire amplification band (for a resolution bandwidth setting of 0.1 nm).

As a comparison, we summarized the performance of the optical amplifier in present work and other available fiber amplifiers, particularly at the wavelength of 1650 nm. Compared with other optical amplifiers, the TDFA we developed exhibits a higher small signal gain (16.5 dB) and lower NF (4.4 dB). Whist the BDGF amplifier and Raman amplifier have a higher gain efficiency, the required fiber lengths of BDGF and Raman fiber are significantly longer than those of TDFAs. Considering the achieved high gain efficiency in fluoride glass based TDFA, further improvements in short wavelength amplifier performance of our developed TDFA are to be expected: there is a considerable scope for further optimization of the passive fiber components and reduction in the splice loss between the active and passive fibers. Furthermore, it is also likely that a further blue shift in the emission cross-section in the $^3F_4$-$^3H_6$ transition will be possible through optimization of the Tm_2O_3 and Ge_2O_3 doping concentrations). In addition, further optimization of pumping schemes could be realized to improve TDFA gain efficiency (better still using a different choice of pump wavelength, i.e. 793 nm pumping which offers a much stronger pump absorption and hence pump rate as opposed to 1550 nm pumping (as previously investigated theoretically in [22])).

3.2 Short wavelength operation of TDFL

To realize short-wavelength operation of the TDFL operating on the $^3F_4$-$^3H_6$ transition, we proposed an all-fiber low-loss cavity as shown in Fig. 5 (a). The linear cavity fiber laser configuration is constructed from ~4.5 m of Ge/Tm co-doped fiber and two tunable FBGs. Due to the high insertion loss of the WDM coupler in Fig. 4(a), it was replaced with a compressively tunable FBG1 with a central wavelength of 1675 nm, which was directly spliced to the input end of the gain fiber. Given that the FBG is highly wavelength selective, it was possible to couple the 1565 nm pump power through the FBG without introducing additional loss. A second identical high reflectivity FBG (FBG2) serves as a low-loss laser cavity mirror as well as an ASE filter to improve performance at wavelengths below 1660 nm. A 15 m long dispersion compensating fiber (DCF, Thorlabs DCF38) wound on a mandrel at an optimized bend diameter of 5.5 cm was added as an additional ASE filter to suppress parasitic lasing at long wavelengths [16]. Tuning of the laser cavity was realized by simultaneously compressing the two FBGs (mounted on mechanical stages) whilst ensuring precise wavelength alignment between the two. The 10 % port of the 90/10 tap coupler was used to extract the output from the TDFL.
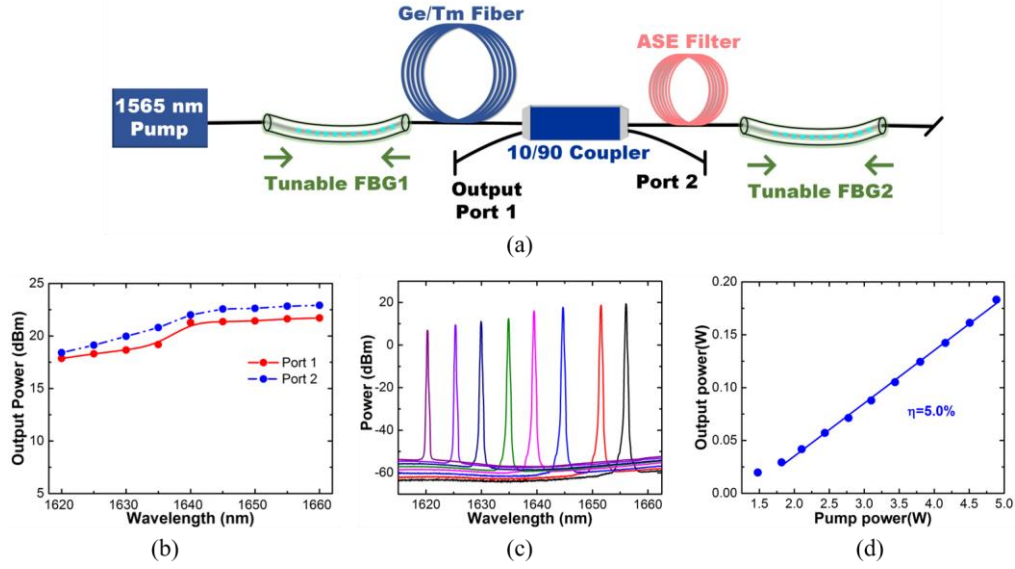
Fig. 5. (a) Schematic of the tunable TDFL, (b) output power of the tunable TDFL at different lasing wavelengths, (c) output spectra of the tunable TDFL (measured with 0.1 nm OSA resolution) and (d) slope efficiency at 1660 nm at port 1.

Figure 5(b) shows the output power as a function of operating wavelength for the maximum available pump power (5W). The highest output power of ~22 dBm was obtained at a wavelength of 1660 nm from port 2 of the 10/90 tap coupler. The shortest lasing wavelength was measured to be 1620 nm with an output power of 17.9 dBm. The output power shows a maximum power variation of 4.5 dB over the entire tuning range from 1620 nm to 1660 nm which signifies the importance of avoiding passive components whose insertion loss varies with wavelength (e.g. WDM coupler). We found that the laser output at port 1 of the coupler exhibits a relatively high optical signal to noise ratio (OSNR) compared to that at port 2. This is because the port 1 output was extracted just after reflection from FBG2 meaning that the out-of-band ASE was well suppressed, resulting in a high OSNR albeit at a slightly lower output power (~2 dB less). Figure 5(c) shows the spectral characteristics of our tunable TDFL. An OSNR of more than 45 dB was successfully achieved across the full tuning range from 1620 nm to 1660 nm (up to 60 dB OSNR from 1640 nm to 1660 nm), and the wavelength of 1620 nm is the shortest wavelength we could reach with the current tunable grating. The 3 dB bandwidth of the laser lines were measured to be < 0.3 nm. The plot in Fig. 5(d) shows the output power at 1660 nm from port 1 as a function of launched pump power. A maximum output power of about 22 dBm was recorded with a slope of efficiency of 5.0 %. When the output power at port 2 taken into account, the internal slope efficiency is ~13.9%. We believe that the output power and lasing efficiency could be further improved by optimizing the ASE filter to provide a much sharper wavelength cutoff and optimizing the composition of the Tm^{3+}-doped germanosilicate glass.

4. Conclusion

By exploiting the Ge/Tm co-doped fiber, we have achieved substantial gain enhancement at the short wavelength edge of the thulium emission band, from 1620 nm to 1660 nm. By constructing a double pass amplifier configuration, we have demonstrated a silica-based TDFA operating from 1628 nm to 1655 nm, a ~2 THz gain bandwidth extension compared to the previous best report. Up to 19 dB small signal gain (external) and a NF as low as 4.4 dB were achieved at 1655 nm. Using two high reflectivity FBGs as cavity mirrors, we have also demonstrated an all-fiber tunable TDFL operating over the 1620-1660 nm wavelength range, providing more than 17.9 dBm output power and >45 dB OSNR over the entire tuning range.

We have experimentally demonstrated that Tm/Ge co-doped fiber provides great potential to improve the short wavelength gain in Tm-doped silica-based fibers and has allowed us to bridge the previous gap between the emission bands of erbium and thulium. Given the quantum defect limit of >90% between pump wavelength and operating wavelengths below 1660nm, we believe there is significant room for improving the laser slope efficiency of silica-based TDFLs and performance of TDFAs at ultra-short wavelengths through this approach. In this work, although we have only reported an internal efficiency of ~13.9%, we are confident that we can increase the figure closer to the quantum limit through composition optimization and further exploring alternative co-dopants. This should ultimately enable much fuller use of the long wavelength edge of the transmission window offered by silica fiber by providing viable silica based rare earth doped fiber amplifiers from just below the C-band out to beyond 2000 nm.

Acknowledgments

References

[1]   S. D. Jackson, "Towards high-power mid-infrared emission from a fibre laser," Nat. Photonics **6**(7), 423–431 (2012).

[2]   C. Crotti, F. Deloison, F. Alahyane, F. Aptel, L. Kowalczuk, J.M. Legeais, D. A. Peyrot, M. Savoldelli, and K. Plaman, "Wavelength optimization in femtosecond laser corneal surgery," Invest. Ophthalmol. Vis. Sci. **54**(5), 3340–3349 (2013).

[3]   N. G. Horton, K. Wang, D. Kobat, C. G.Clark, F. W.Wise, C. B. Schaffer and C. Xu, "In vivo three-photon microscopy of subcortical structures within an intact mouse brain," Nat. Photonics **7**(3), 205–209 (2013).

[4]   U. Sharma, E. W. Chang, and S. H. Yun, "Long-wavelength optical coherence tomography at 1.7 µm for enhanced imaging depth," Opt. Express **16**(24), 19712–19723 (2008).

[5]   P. Cadroas, L. Abdeladim, L. Kotov, M. Likhachev, D. Lipatov, D. Gaponov, A. Hideur, M. Tang, J. Livet, W. Supatto, E. Beaurepaire, and S. Février, "All-fiber femtosecond laser providing 9 nJ, 50 MHz pulses at 1650 nm for three-photon microscopy," J. Opt. **19**(6),2017.

[6]   T. Delahaye, S. E. Maxwell, Z. D. Reed, H. Lin, J. T. Hodges, K. Sung, V. M. Devi, T. Warneke, P. Spietz, and H. Tran, "Precise methane absorption measurements in the 1.64 µm spectral region for the MERLIN mission," J. Geophys. Res. Atmos. **121**, 7360–7370 (2016).

[7]   D. F. Siriani, J. J. Plant, T. J. Garrod, A. Napoleone, S. Mouser, and P. W. Juodawlkis, "High-Power 1.65 µm Slab-Coupled Optical Waveguide Amplifiers," in CLEO, JTu5A.100 (2017).

[8]   B. Niu , H. Yu , L. Yu , D. Zhou , D. Lu , L. Zhao , J. Pan, and W. Wang, "1.65 µm three-section Distributed Bragg Reflective (DBR) laser for CH_4 gas sensor," J. Semicond. **34**(10), 104004 (2013).

[9]   S. V. Firstov, S. V. Alyshev, K. E. Riumkin, V. F. Khopin, A. N. Guryanov, M. A. Melkumov, and E. M. Dianov, "A 23-dB bismuth-doped optical fiber amplifier for a 1700-nm band," Sci. Rep. **6**(1), 28939–28946 (2016).

[10]   C. Kakkar, G. Monnom, K. Thyagarajan, and B. Dussardier, "Inherently gain flattened L+band TDFA based on W-fiber design," Opt. Commun. **262**(2), 193–199 (2006).

[11]   M. Yamada, K. Senda, T. Tanaka, Y. Maeda, S. Aozasa, H. Ono, K. Ota, O. Koyama, and J. Ono, "Tm^{3+}–Tb^{3+}-doped tunable fibre ring laser for 1700 nm wavelength region," Electron. Lett. **49**(20), 1287–1288 (2013).

[12]   J. M. O. Daniel, N. Simakov, M. Tokurakawa, M. Ibsen, and W. A. Clarkson, "Ultra-short wavelength operation of a thulium fibre laser in the 1660–1750 nm wavelength band," Opt. Express **23**(14), 18269(2015).

[13]   W. L. Barnes and J. E. Townsend, "Highly tunable and efficient diode pumped operation of Tm^{3+}-doped fiber lasers," Electron. Lett. **26**(11), 746–747 (1990).

[14]   S. D. Agger and J. H. Povlsen, "Emission and absorption cross section of thulium doped silica fibers," Opt. Express **14**(1), 50 (2006).

[15]   Y.Jung, Z. Li, N. Simakov, J. M. O. Daniel, D. Jain, P. C. Shardlow, A. M. Heidt, J. K. Sahu, A. Hemming, W. A. Clarkson, S.U. Alam, and D.J. Richardson, "Silica-based thulium doped fiber amplifiers for wavelengths beyond the L-band," Opt. Fiber Commun. Conf. *(OFC)*, M3D.5 (2016).

[16]   Z. Li, Y.Jung, J. M. O. Daniel, N. Simakov, M. Tokurakawa, P.C. Shardlow, D. Jain, J.K. Sahu, A.M. Heidt, W. A Clarkson, S.U. Alam, and D.J. Richardson, "Exploiting the short wavelength gain of silica-based thulium-doped fiber amplifiers," Opt. Lett. **41**(10), 2197 (2016).

[17]   A. Sincore, J. D. Bradford, J. Cook, L. Shah, and M. C. Richardson, "High Average Power Thulium-Doped Silica Fiber Lasers: Review of Systems and Concepts," IEEE J. Sel. Top. Quantum Electron. **24**(3), 1–8

(2018).

[18] D. A. Simpson and G. Baxter, "Spectroscopy of Thulium Doped Silica Glass,"*PhD thesis*,181(2007).

[19] D.E.McCumber, "Theory of Phonon-Terminated Optical Masers," Phys. Rev. **134**(2A), 299-306 (1964).

[20] R. Li, C. Tian, Y. Tian, T. Wei, B. Li, X. Jing, F. Ruan, and F. Wang, "Mid-infrared emission properties and energy transfer evaluation in Tm^{3+}-doped fluorophosphate glasses," J. Lumin. **162**, 58–62 (2015).

[21] M. R. Mokhtar, C. S. Goh, S. A. Butler, S. Y. Set, K. Kikuchi, D. J. Richardson, and M. Ibsen, "Fibre Bragg grating compression-tuned over 110nm," Electron. Lett. **39**(6), 509–511(2003).

[22] J. Yang, H. Zhong, S. Zhang, and D. Fan, "Theoretical Characterization of the Ultra-Broadband Gain Spectra at ∼1600-2100 nm from Thulium-Doped Fiber Amplifiers," IEEE Photonics J. **8**(6), 1400310 (2016).